HHS Public Access

Author manuscript

Matrix Biol. Author manuscript; available in PMC 2018 July 01.

Published in final edited form as:

Matrix Biol. 2017 July ; 60-61: 190–205. doi:10.1016/j.matbio.2016.11.008.

Breast Cancer-Derived Extracellular Vesicles Stimulate Myofibroblast Differentiation and Pro-Angiogenic Behavior of Adipose Stem Cells

Young Hye Song[1], **Christine Warncke**[1], **Sung Jin Choi**[1], **Siyoung Choi**[1], **Aaron E. Chiou**[1], **Lu Ling**[1], **Han-Yuan Liu**[2], **Susan Daniel**[2], **Marc A. Antonyak**[3], **Richard A. Cerione**[3,4], and **Claudia Fischbach**[1,5,*]

[1]Nancy E. and Peter C. Meinig School of Biomedical Engineering, Cornell University, Ithaca, NY

[2]Robert Frederick Smith School of Chemical and Biomolecular Engineering, Cornell University, Ithaca, NY

[3]Department of Molecular Medicine, Cornell University, Ithaca, NY

[4]Department of Chemistry and Chemical Biology, Cornell University, Ithaca, NY

[5]Kavli Institute at Cornell for Nanoscale Science, Cornell University, Ithaca, NY

Abstract

Adipose-derived stem cells (ASCs) are abundantly present in the mammary microenvironment and can promote breast cancer malignancy by differentiating into myofibroblasts. However, it remains largely unclear which role tumor-derived extracellular vesicles (TEVs) play in this process. Here, we used microfabricated, type I collagen-based 3-D tissue culture platforms to investigate the effect of breast cancer cell-derived TEVs on ASCs myofibroblast differentiation and consequential changes in extracellular matrix remodeling and vascular sprouting. TEVs collected from MDA MB-231 human metastatic breast cancer cells (MDAs) promoted ASC myofibroblast differentiation in both 2-D and 3-D culture as indicated by increased alpha smooth muscle actin (α-SMA) and fibronectin (Fn) levels. Correspondingly, TEV-treated ASCs were more contractile, secreted more vascular endothelial growth factor (VEGF), and promoted angiogenic sprouting of human umbilical vein endothelial cells. These changes were dependent on transforming growth factor beta (TGF-β)-related signaling and tumor cell glutaminase activity as their inhibition decreased TEV-related myofibroblastic differentiation of ASCs and related functional consequences. In summary, our data suggest that TEVs are important signaling factors that contribute to ASC desmoplastic reprogramming in the tumor microenvironment, and suggest that tumor cell glutamine metabolism may be used as a therapeutic target to interfere with this process.

*corresponding author: Claudia Fischbach-Teschl, 157 Weill Hall, Cornell University, Ithaca, NY 14850, cf99@cornell.edu.

Keywords

tumor microvesicles; extracellular matrix; adipose-derived stem cells; myofibroblast; fibronectin; angiogenesis

1. Introduction

Excessive fibrotic remodeling of the stroma, termed desmoplasia, is a hallmark of breast cancer that is mediated by myofibroblasts and correlates with an advanced, invasive phenotype and worse clinical prognosis[1–3]. Myofibroblasts are highly contractile cells that contain alpha smooth muscle actin (α-SMA)-positive stress fibers[4] and are able to deposit and remodel key fibrillar components of the extracellular matrix (ECM) including type I collagen and fibronectin[5,6]. The resulting compositional, structural, and mechanical changes of the ECM directly impact tumor cell aggressiveness[7–9]. Increasing evidence also suggests that myofibroblasts play a critical role in regulating tumor angiogenesis, i.e., the formation of new blood vessels from a pre-existing vasculature necessary for tumor growth and metastasis[10–12]. More specifically, myofibroblasts can promote vascular sprouting directly and indirectly through their secretion of key pro-angiogenic factors including vascular endothelial growth factor (VEGF) and their ECM remodeling capability, respectively[13].

While fibroblasts and bone marrow-derived mesenchymal stem cells are typically discussed as the main cellular source of myofibroblasts[14,15], adipose-derived stem cells (ASCs) may be similarly important[16]. ASCs are abundantly contained in mammary fat, but can also circulate in the blood stream and thus be recruited to mammary tumors from distant sites[17]. In fact, breast cancer-associated ASCs can differentiate into myofibroblasts[18] as detected by increased expression of α-SMA[19], greater contractility[20], and elevated deposition of fibrillar ECM proteins[21,22]. Additionally, ASCs have also been shown to modulate angiogenesis through various mechanisms. For example, ASCs secrete pro-angiogenic factors such as VEGF, associate perivascularly with blood vessels, and provide physical ECM guidance cues that promote endothelial sprouting[13,23,24]. Collectively, these changes render the tumor microenvironment more permissive for further progression towards malignancy (22). However, the signaling mechanisms by which tumors transform ASCs into myofibroblasts and the resulting consequences on endothelial cell invasion and subsequent tumor angiogenesis remain poorly understood.

Tumor cell-derived extracellular vesicles (TEVs) including exosomes and microvesicles (MVs) are increasingly recognized for their role in tumorigenesis and appear to also play a role in myofibroblast differentiation, but their effects on ASCs remain unclear. Exosomes are released from late endosomal multivesicular bodies[25], whereas MVs are generated by outward budding and pinching off of the plasma membrane and at greater levels by more malignant cancer cells[26]. Once thought to be cellular debris, these TEVs contain a variety of signaling molecules that prime the host microenvironment for tumor progression[27–30]. More specifically, TEVs not only facilitate the evasion of immune responses and drug therapy, but also support the establishment of pre-metastatic niches[31–33]. TEVs have also

been shown to promote myofibroblastic differentiation of stromal progenitor cells[34,35]. Specifically, enhanced potency of TEV-associated transforming growth factor beta (TGF-β), a key driver of myofibroblast differentiation[36], has been correlated with increased myofibroblastic behavior of fibroblasts[37].

The goals of this study were to i) assess whether TEVs play a role in breast cancer-associated differentiation of ASCs into myofibroblasts and ii) if the resulting phenotypic differences functionally impact endothelial sprouting. Using 2-D and 3-D cell culture approaches, our work suggests that ASC phenotypic changes in a tumor-like microenvironment are mediated by TEVs and that therapeutic intervention with this process may be used to deter ASC-mediated changes in tumor stroma remodeling and thus, overall tumor malignancy.

2. Results

2.1. Breast cancer cells secrete extracellular vesicles

To characterize extracellular vesicles (EVs) shed by MDA MB-231 human breast cancer cells (MDAs), MDAs were incubated with serum-free culture media and tumor cell-derived extracellular vesicles (TEVs) were isolated from the conditioned media via size-based filtration (Fig. 1A). Subsequently, NanoSight®, a nanoparticle tracking analysis tool, and Zetasizer, a dynamic light scattering tool, were used to measure particle size concentration and distribution of isolated TEVs. EVs shed by ASCs were collected similarly and served as a control to confirm increased EV biogenesis by malignant vs. normal cells. Indeed, MDAs produced significantly greater levels of EVs than ASCs, and negligible numbers of particles were detected in the respective serum-free control media (Figs. 1B, C). Additionally, the particle size distribution of TEVs was markedly different from that of blank control media (Figs. 1D, E). These results imply that MDAs secrete significantly more EVs than ASCs, further supporting previous studies suggesting that EV production positively correlates with cell malignancy[26,38].

2.2. TEVs drive myofibroblastic differentiation of ASCs in 2-D

While cancer cell-derived paracrine signals are generally known to promote the differentiation of host stromal cells into myofibroblasts[5,39], it remains unknown which specific role TEVs play in this process. To investigate the effect of TEVs on ASC myofibroblast differentiation, ASCs were treated with MDA-shed TEVs and their expression of the myofibroblast markers alpha smooth muscle actin (α-SMA) and fibronectin was analyzed. Indeed, TEV-treated ASCs increased their expression of α-SMA, as evidenced by both immunofluorescence (Figs. 2A, B) and Western blot analysis (Fig. 2D). Additionally, TEV-treated ASCs assembled fibronectin matrices that were more abundant and composed of thicker fibers relative to those deposited by control ASCs (Fig. 2C). This suggests that TEV treatment enhances hallmark features of myofibroblastic differentiation in ASCs.

2.3. TEVs activate MAPK signaling pathways in ASCs

It is well established that tumor cell-secreted transforming growth factor-beta (TGF-β) drives myofibroblastic differentiation[18,40], and that TGF-β-mediated activation of the

mitogen-activated protein kinases (MAPK) pathway contributes to this process[41,42]. Interestingly, TEVs also contain TGF-β[37], but whether TEVs promote ASC myofibroblast differentiation through activating the MAPK signaling cascade remains unclear. To address this question, ASCs were treated for one hour with TEVs and the resulting consequences on the phosphorylation levels of the MAPK family members ERK1/2 and JNK1/2 were measured. ASC-treatment with TEVs stimulated phosphorylation of ERK1/2 and JNK1/2, and this effect was inhibited by prior neutralization of TEV-associated TGF-β using a function-blocking antibody (Figs. 3A, B). Consistent with these findings, addition of a TGF-β neutralizing antibody or the JNK2 inhibitor SP600125 decreased ASC myofibroblast differentiation in response to TEV treatment as indicated by significantly reduced α-SMA levels (Figs. 3C, D). Interestingly, addition of the MEK inhibitor PD98059 did not affect α-SMA levels of ASCs, and fibronectin levels did not change in response to either SP600125 or PD98059 (data not shown). Collectively, these data suggest that TEVs activate MAPK signaling pathways in ASCs in a TGF-β-dependent manner and that these changes contribute to the TEV-induced myofibroblast differentiation of ASCs.

2.4. TEVs drive myofibroblastic differentiation of ASCs in 3-D

Given that cellular behavior is strongly influenced by culture context (dimensionality, substrate mechanical properties etc.), we next assessed whether TEV-mediated changes in ASC phenotype also occurred under physiologically more relevant culture conditions. To this end, ASCs were embedded in type I collagen, an ECM component present in the native ASC microenvironment[43,44], and cultured in the presence and absence of TEVs. These 3-D hydrogels were microfabricated to sizes below the diffusion limit of oxygen and nutrients (~200 μm) to ensure that results were not due to varied solute transport. Two different 3-D culture systems were used: free-floating disks to measure cell contractility via changes in surface area, and poly(dimethylsiloxane) (PDMS)-based microwells that permit analysis of cell-cell interactions in both homo- and heterotypic cell culture using 3-D confocal imaging (Fig. 4A). Similar to 2-D cultures, TEV treatment increased α-SMA and fibronectin levels of ASCs in 3-D microwell cultures (Figs. 4B, C). To investigate the functional consequences of TEV-driven increases in α-SMA levels, ASC contractility was assessed by embedding the cells in free-floating 3-D type I collagen and measuring hydrogel contraction following culture with and without TEVs. Indeed, TEV-treated ASCs contracted the gels significantly more than control cells (Figs. 4D, E). These data suggest that TEVs induce myofibroblastic differentiation of ASCs in 3-D culture and consequential profibrotic ECM remodeling.

2.5. Glutaminase inhibition reduces TEV generation by MDAs

Altered glutamine metabolism has been implicated in TEV biogenesis by cancer cells[45]. Specifically, elevated activity of mitochondrial glutaminase has been linked to both increased malignant potential of breast cancer cells and TEV production[46]. To confirm the role of glutaminase in regulating TEV release by MDAs, a small molecule glutaminase inhibitor, Compound 968, was added to MDAs prior to TEV collection (Fig. 5A). Morphological analysis of MDAs using SEM indicated that control cells were characterized by extensive bulging of their cell membranes indicative of TEV biogenesis (Fig. 5B). In contrast, MDAs exhibited smooth cell surfaces following 968 treatment, with no presence of outbudding TEVs. Accordingly, NanoSight analysis indicated that media harvested from

968-treated MDAs showed a significant decrease in particle counts relative to media harvested from MDA control cells (Figs. 5C, D). Analysis of 968-containing media alone showed no significant difference relative to blank control media. Further analysis with Zetasizer revealed smaller particle distribution in 968-TEVs compared to TEVs (Fig. 5E). These data suggest that glutaminase-inhibition in tumor cells using Compound 968 may be used to interfere with the TEV-mediated transformation of tissue-resident ASCs.

2.6. Inhibition of TEV formation reduces myofibroblastic differentiation of ASCs

To test whether reduction of TEV production with Compound 968 can reverse the TEV-mediated myofibroblastic differentiation of ASCs, phosphorylated and total ERK1/2 and JNK1/2 levels of ASCs were measured. Indeed, the TEV fraction collected from 968-treated MDAs, hereby labeled 968-TEV, did not induce phosphorylation of ERK1/2 and JNK1/2 in ASCs (Figs. 6A, B). Consequently, changes in α-SMA levels were also detected by Western blot (Figs. 6C, D). Additionally, ASCs decreased their expression of α-SMA and fibronectin in 3-D collagen microwells upon 968-TEV *vs.* TEV treatment (Figs. 6E, F). Furthermore, cell contractility was decreased upon treatment with 968-TEVs, as demonstrated by reduced collagen gel contraction relative to treatment with TEVs that were collected in the absence of 968 (Figs. 6G, H). Using previously developed method to assess proteolytic ECM remodeling by ASCs[24], collagen matrix degradation profile showed larger pores generated by TEV treated ASCs compared to control media and 968-TEV treated ASCs (Figs. 6I, J). Collectively, these data suggest that myofibroblastic differentiation of ASCs in a mammary tumor-like microenvironment relies on the glutaminase-dependent biogenesis of TEVs, and that interfering with glutaminase is a potential strategy to prevent stroma remodeling by myofibroblastic ASCs in the mammary tumor microenvironment.

2.7. TEVs enhance ASC pro-angiogenic behavior and consequential endothelial sprouting

Myofibroblasts are highly pro-angiogenic and recruit endothelial cells to increase tumor vascularization[11,47]. To investigate whether TEVs promote the pro-angiogenic capability of ASCs, their secretion of vascular endothelial growth factor (VEGF) was measured. Indeed, TEV treatment increased VEGF secretion by ASCs relative to control media, and this effect was not observed when ASCs were cultured with 968-TEVs (Fig. 7A). These results suggest that glutaminase-dependent biogenesis of TEVs by MDAs promotes VEGF secretion by ASCs.

To assess whether the detected increase of VEGF secretion by ASCs is functionally relevant to angiogenesis, vascular sprouting of human umbilical vein endothelial cells (HUVECs) into collagen gels containing either TEV-pretreated ASCs or control ASCs was investigated. These experiments were performed with a modified version of the above-described 3-D collagen-based microwell platform (Fig. 7B), which mimics interactions of ASCs with an adjacent endothelium and allows studying 3-D vascular invasion using confocal image analysis. TEV-treated ASCs increased HUVEC sprout formation, and this effect was reduced upon 968-TEV treatment (Figs. 7C, D). Blank gels incubated with TEVs did not elicit angiogenic sprouting by HUVECs, suggesting that the endothelial sprouts were induced by altered ASC behavior rather than TEVs that may have been sequestered during the pre-incubation period (Fig. 7D). To verify that TEV-mediated differences of VEGF

secretion by ASCs contributed to the detected differences in angiogenic sprouting, a VEGF neutralizing antibody (α-VEGF) was added to the different ASC-HUVEC co-cultures. VEGF inhibition significantly reduced HUVEC sprouting under conditions in which ASCs were pre-treated with TEVs; a less pronounced, but still significant decrease was also noted for 968-TEV pretreated ASCs, whereas no significant differences were detected for ASCs pre-treated with control media (Fig. 7E). These results suggest that TEV-conditioned ASCs increased HUVEC sprout formation through their increased secretion of VEGF. Additionally, to specifically determine whether TEV-dependent changes of ECM remodeling by ASCs, a phenomenon previously shown to modulate angiogenic sprouting[24], contributed to our observations, experiments were repeated following detergent-based decellularization of collagen microwells. ASCs pretreated with TEVs promoted endothelial cell sprouting and this effect was maintained following decellularization (Fig. 7F). Finally, combining decellularization with VEGF inhibition significantly decreased HUVEC sprouting in collagen matrices preconditioned by TEV-treated ASCs, whereas this effect was not observed in microwells that were preconditioned by control ASCs (Figs. 7G, H). These results suggest that TEV-dependent changes in ASC-mediated ECM remodeling as well as consequential changes in VEGF sequestration play a role in modulating endothelial sprouting. In summary, TEVs enhance the pro-angiogenic capabilities of ASCs by increasing both their secretion of VEGF and ECM remodeling.

3. Discussion

Paracrine signaling between cancer cells and host stromal cells supports the formation of a tumor-promoting microenvironment by increasing desmoplasia and tumor angiogenesis. However, the integrated contributions of ASCs and TEVs to these changes remain elusive. Using both 2-D and 3-D culture systems that allow quantitative assessment of cell- and tissue-level phenomena, we show that TEVs promote myofibroblastic differentiation of ASCs in a manner that depends on tumor cell glutamine metabolism. Moreover, our data suggest that these changes increase endothelial sprouting by modulating both VEGF secretion and ECM remodeling by ASCs.

Our finding that the pro-myofibroblastic effects of MDA-derived TEVs could be inhibited by blocking glutaminase is exciting as this identifies a novel therapeutic target to interfere with desmoplasia. In general, many cancer cells are glutamine-addicted in order to satisfy their increased biosynthetic needs for proteins, lipids, and nucleotides as well as to maintain mitochondrial function, and glutaminase is a key enzyme of this metabolic pathway[48]. The commercially available glutaminase inhibitor Compound 968 functions by preventing active tetramer formation of glutaminase[49] and has been linked to suppression of RhoA-mediated cell contractility, which controls shedding of MVs into the extracellular space[50]. However, it should be considered that glutaminase inhibition not only limits TEV biogenesis, but can also affect other mechanisms. For example, 968 treatment of MDAs can change gene expression, histone modification, apoptosis, and sensitivity to drug treatment[51]. Additionally, MDAs treated with 968 exhibit decreased malignant behavior relative to control cells[46]. Given these effects of 968 on MDAs, it is possible that 968 treatment may also modulate the function of the residual MVs and that these effects contribute to the detected changes in ASC behavior. Future studies will need to evaluate

whether these changes could independently affect the ability of MDAs to promote desmoplasia and if other mesenchymal and patient-derived cells respond similarly. Yet glutaminase inhibitors and other pharmacological inhibitors against glutamine metabolism have demonstrated success in both pre-clinical and clinical trials. Hence, our findings may contribute to a better understanding of these outcomes[52].

It is also worth noting that 968 treatment is unlikely to interfere with exosome biogenesis as exosomes are generated through a different mechanism; i.e., exocytosis of endosomal multivesicular bodies with the plasma membrane rather than RhoA-mediated, actomyosin based pinching of the plasma membrane[25,53]. While the data presented herein imply that 968-induced inhibition of TEV production is sufficient to reverse phenotypic changes of ASCs, the link between glutaminase inhibition and exosome release remains to be investigated. Current knowledge of the difference between MVs and exosomes are limited to their size distribution and mechanism of formation[54], but whether or not they exhibit differential capacities to promote desmoplasia and tumor angiogenesis remains unclear. Further analysis of the two populations of EVs, such as mechanism of cargo sorting and transfer into recipient cells, is necessary in order to gain a better understanding of their contribution to disease progression. Myofibroblasts are key regulators of tumor desmoplasia and originate not only from host resident fibroblasts, but also mesenchymal stem cells such as ASCs[55]. Our work suggests that TEVs stimulate ASCs to undergo differentiation into myofibroblasts as demonstrated by their increased levels of α-SMA and fibronectin, enhanced cell contractility and generation of larger degradation pores throughout the matrices.

Myofibroblastic differentiation was reduced when ASCs were treated with 968-TEVs, alluding to a functional link between tumor cell glutamine metabolism, TEV biogenesis, and transformation of stromal cells. Although treatment with 968 did not fully inhibit TEV biogenesis by MDAs as demonstrated by NanoSight and Zetasizer analyses, it is possible that the TEVs shed by 968-treated MDAs are less potent to exert their effects on ASCs. Furthermore, it should be considered that TEV treatment may not only increase the quantity of fibronectin deposition as suggested by our studies, but also alter nano- and microstructural features of the deposited fibronectin matrix[21,22]. These changes may, in turn, indirectly affect the proangiogenic functions of ASCs[21,56].

In addition to increasing α-SMA and fibronectin levels, TEVs increased ERK and JNK phosphorylation by ASCs, a response that was attenuated upon treatment with 968-TEV or a function-blocking TGF-β antibody. TGF-β is known to activate not only its canonical Smad2/3 pathways, but also MAPK signaling, and these changes may contribute to our findings[42]. For example, activation of p38 by TGF-β1 is required for myofibroblastic differentiation of human fetal lung fibroblasts[41], and TGF-β-dependent ERK and JNK activation has been shown to increase α-SMA expression[57,58]. However, in our studies, only inhibition of JNK phosphorylation decreased TEV-dependent changes of α-SMA, while ERK inhibition had no effect. This suggests that increased ERK phosphorylation may have been a consequence rather than requirement for TEV-mediated ASC transformation in our experimental settings. Furthermore, neither ERK nor JNK inhibition impacted fibronectin levels, which may be explained by a recent study showing that TGF-β can

modulate α-SMA levels of myofibroblast precursors independent of pre-existing or newly deposited fibronectin[59]. Interestingly, previous work using periodontal ligament fibroblasts indicated that ERK and JNK phosphorylation can also negatively correlate with myofibroblastic differentiation[60] and that bFGF-mediated ERK phosphorylation correlates with lower levels of α-SMA in ASCs[61]. Hence, it will be important to assess the contribution of other TEV cargo molecules to ASC myofibroblastic differentiation and MAPK pathway activation and to determine the *in vivo* relevance of our findings in the mammary tumor microenvironment.

TEV treatment of ASCs increased angiogenic invasion from an adjacent HUVEC monolayer. Sprout formation was reduced when ASCs were treated with 968-TEVs rather than TEVs, suggesting that TEV-mediated transformation of ASCs affected not only their myofibroblastic differentiation but also their pro-angiogenic capability. Importantly, TEV-treated ASCs induced angiogenic sprouting not only by secreting more VEGF, but also by altering the ECM. More specifically, experiments with decellularized ECMs revealed that endothelial cells invaded more readily into matrices remodeled by TEV-treated *vs.* control ASCs. These findings are consistent with previous results suggesting that ASCs can generate physical guidance channels that encourage vascular invasion[24] and that deposition of fibronectin within these spaces may promote sprouting[62]. Nevertheless, blockade of VEGF signaling with a neutralizing antibody decreased endothelial sprouting in decellularized microwells, implying that ECM-sequestered VEGF also contributed to our observations.

Although the work described here focused on TEVs derived from malignant breast cancer cells, stromal remodeling in the mammary microenvironment occurs gradually during disease progression and even in the absence of tumors as in the case of obesity[44]. It would be interesting to compare the effect of EVs isolated from normal, premalignant, and malignant mammary epithelial cells on ASCs and to determine if the resulting changes in ASC pro-angiogenic and ECM remodeling capabilities are similar in magnitude to those mediated by cancer-associated fibroblasts (CAFs)[5]. Whether or not TEV treatment increases EV production of the ASCs themselves would be another aspect worth addressing as such EVs may further promote tumorigenesis[63]. While our study has focused on the role of MAPK signaling in TEV-mediated differences of ASC myofibroblast differentiation, TGF-β-dependent activation of the Smad2/3 pathway is likely to play an important role as well[4]. Furthermore, previous reports have suggested that vesicular TGF-β is more potent relative to free TGF-β[37], a phenomenon that may have contributed to our results and warrants further investigation. Additionally, the culture models used in our studies lend themselves to mechanical characterization and will allow assessing the effect of TEV-treated ASCs on ECM stiffening, a hallmark of desmoplasia that permits breast cancer diagnosis via palpation and directly contributes to malignant transformation[3,64,65]. Finally, future studies will need to test whether the detected differences in TEV-mediated changes of ASC proangiogenic capability contribute to the formation of leaky and dilated vessels found in tumors[66]. Such studies can be performed *in vivo*, but would also benefit from microfluidic platforms in which perfusable endothelialized channels can be embedded into ASC-seeded collagen scaffolds and allow generating insights into how TEV-treated ASCs contribute to remodeling of the tumor vasculature[67,68].

In summary, this work suggests that TEVs promote myofibroblastic differentiation and pro-angiogenic behavior of ASCs, and that these changes contribute to increased vascular sprouting. Interestingly, this effect was dependent on tumor cell glutamine metabolism, as blocking glutaminase inhibited TEV formation and consequential changes in ASC behavior. Hence, interfering with glutaminase may be used as a potential therapeutic strategy to reduce TEV-mediated changes of desmoplasia and tumor angiogenesis in the future.

4. Experimental Procedures

4.1. Cell culture

Human ASCs were purchased from Lonza, routinely cultured in growth media (ADSC-GM, Lonza) and utilized between passages 3 to 6. Human breast adenocarcinoma cells MDA MB-231 (MDAs) were purchased from ATCC and maintained in their growth media containing minimum essential medium with alpha modification (α-MEM, Sigma) supplemented with 10% fetal bovine serum (FBS, Atlanta Biologicals) and 1% penicillin/streptomycin (P/S, Gibco). Human umbilical vein endothelial cells (HUVECs, Lonza) were expanded in growth media (HUVEC-GM) composed of Bio-Whittaker® Media 199 (M199, Lonza) supplemented with 16% FBS, 1% P/S, 30 μg/mL endothelial cell growth supplement (Millipore), 2 mM Glutamax (Gibco), and 2500 U heparin sulfate sodium salt (Sigma). For experiments, HUVECs were used between passages 3 and 4. Cell cultures were maintained at 37°C, 5% CO_2 with media changes every 2 days.

4.2. Extracellular vesicle isolation and glutaminase inhibition

MDAs were maintained in their growth media until 80–90% confluency, at which time they were incubated with serum-free α-MEM for 7–12 hours (Fig. 1A). Control media; i.e., serum-free α-MEM, was treated similarly in the absence of cells. For glutaminase inhibition studies, MDAs were treated with 10 μM Compound 968 dissolved in DMSO (Millipore), a small molecule inhibitor against mitochondrial glutaminase, in growth media. As a control to 968, an equal volume of DMSO was added to media prior to incubation with cells. After 24 hours, MDAs were rinsed with PBS and incubated with serum-free α-MEM with compound 968, also for 7–12 hours. Media were harvested and centrifuged twice to remove cell debris. EVs were isolated by slow vacuum filtration through 0.22 μm membrane filters (Millipore) or 100,000 MWCO concentration filter centrifugal tubes (Millipore), and subsequently rinsed with serum-free α-MEM. The concentrated media were reconstituted in Dulbecco's minimum essential medium (DMEM, Gibco) mixed with F-12 nutrient mixture (Gibco) supplemented with 1% FBS and 1% P/S (DMEM/F12) for ASCs, with fresh EVs isolated for every media change. For size and concentration measurement, enriched EVs were analyzed with NanoSight and Zetasizer (both Malvern). EVs from ASCs were collected similarly, with serum-free DMEM/F12.

4.3. Scanning electron microscopy

To visualize MDAs and EVs, MDAs were cultured on 12 mm micro cover glass (VWR) coated with fibronectin (30 μg/mL, Gibco). After 48 hours of culture, MDAs were treated with or without Compound 968 as described above. After 7 hours of incubation in serum-free media, MDAs were fixed in 2.5% glutaraldehyde (Electron Microscopy Sciences) in 50

mM cacodylate buffer (Electron Microscopy Sciences). Subsequently, MDAs were washed with 50 mM cacodylate buffer, dehydrated using a serial ethanol gradient, treated with hexamethyldisilazane (Electron Microscopy Sciences), and finally air-dried in a chemical fume hood overnight. Samples were attached to SEM specimen mounts using conductive carbon adhesive tabs (Electron Microscopy Sciences), coated with gold/palladium alloy in a sputter coater (Denton Vacuum), and imaged using MIRA3 LM (Tescan) SEM at 5 keV.

4.4. TEV treatment of ASCs

ASCs were cultured in low-serum (1% FBS) DMEM/F12 supplemented with freshly isolated TEVs (4×10^8 particles/mL) or the corresponding control fraction for 7 days. TEVs or the control fraction were replenished with each media change. For 2-D cultures, ASCs were seeded onto fibronectin-coated (30 μg/mL, Gibco) plastic coverslips (Nunc) for immunofluorescence analysis or on tissue culture treated 6-well plates for western blot analysis. For inhibition studies, ASCs were serum starved overnight before treatment with anti-human LAP TGF-β1 blocking antibody (500 ng/mL, R&D Systems), MEK inhibitor PD98059 (10 μM, Millipore), and JNK inhibitor SP600125 (10 μM, Millipore) in the presence of TEVs for 7 days. For 3-D culture, ASCs were grown in rat tail-derived type I collagen hydrogel-based microwells (Fig. 4A-i) and free-floating disks (Fig. 4A-ii) as described previously[24,69]. Briefly, microwells were made with poly(dimethylsiloxane) (PDMS, Dow Corning) using conventional soft lithography approaches (depth: 200 μm; diameter: 4 mm) and free-floating type I collagen disks were prepared using plexiglass molds with circular patterns (depth: 500 μm; diameter: 4 mm). For both 3-D culture systems, blank gels without incorporated ASCs were prepared as controls.

4.5. Endothelial cell invasion assay

For analysis of endothelial cell invasion, a confluent monolayer of HUVECs was seeded on top of the ASC-embedded and TEV-pretreated collagen microwells, as described previously[24]. For decellularization experiment, ASCs were removed via chemical digestion with NH_4OH and Triton-X prior to HUVEC introduction. Success of decellularization was confirmed by lack of DAPI staining. These co-cultures were maintained in low-serum (1%) HUVEC-GM supplemented with 50 mg/mL L-ascorbic acid (Acros Organics) and 50 ng/mL tetradecanoyl phorbol acetate (TPA, Cell Signaling Technology) for 3 days. Subsequently, cultures were fixed and immunofluorescence was performed as described below. For HUVEC sprout quantification, individual CD31-positive sprouts extending a minimum of 10 μm into the bulk of the gel were counted.

4.6. Immunofluorescence

Immunofluorescence analysis was performed as described previously[24]. Briefly, ASCs were fixed in 10% neutral-buffered formalin (Millipore), washed with PBS, permeabilized with Triton-X (VWR), and blocked with bovine serum albumin (Fisher Scientific). ASCs were probed with rabbit anti α-SMA monoclonal antibody (Abcam), while fibronectin deposition was detected without prior permeabilization using a mouse anti-fibronectin monoclonal antibody (Sigma). HUVECs were labeled with a mouse anti-CD31 monoclonal antibody (R&D Systems). Primary antibodies were labeled with host-matching Alexa Fluor® secondary antibodies and cell nuclei and the cytoskeleton were probed with DAPI

and Alexa Fluor® phalloidin (Life Technologies), respectively. Fluorescent images as well as reflectance images of 3-D cultures were imaged using a Zeiss LSM 710 confocal microscope, and 2-D cultures were imaged with an Axio Observer.Z1 Zeiss inverted epifluorescence microscope. For each microscope, the channel settings and the exposure times were kept constant. Quantification of α-SMA and fibronectin levels of ASCs was done using the RGB measurement plugin in ImageJ. The thickness of ASC-deposited fibronectin fibers in 2-D cultures was measured manually in ImageJ. Gel degradation pore area measurements were done using ImageJ, as previously described [24]. Briefly, surface area of the black pores shown in the reflectance channel images was measured.

4.7. Analysis of VEGF secretion by ASCs

To measure VEGF secretion by ASCs, two 3-D microwells were pooled and incubated with DMEM/F12 after 7 days of culture with control or EV-containing media. After 24 hours, conditioned media were harvested and stored at −20°C until analysis by enzyme-linked immunosorbent assay (ELISA, R&D Systems).

4.8. Western blot

ASCs were cultured in 2-D with TEV, 968-TEV or control media for 7 days. For ERK1/2 and JNK1/2 analysis, ASCs were seeded in 10-cm culture dishes and treated with TEVs or other designated media for 1 hour. Subsequently, cells were harvested in RIPA-based lysis buffer (Thermo Scientific). Gels were fabricated using FastCast 7.5% Acrylamide Kit (Bio-Rad). Samples were diluted in Laemmli sample buffer (Bio-Rad) and β-mercaptoethanol (J.T. Baker), run via SDS-PAGE, and transferred onto PVDF membrane (Bio-Rad). The membranes were then blocked and incubated with primary antibodies against α-SMA (Abcam) and fibronectin (Sigma) at 4°C overnight. Hsp90 was probed as a loading control (Santa Cruz Biotechnology). After subsequent washing steps, the membranes were probed with HRP-conjugated secondary antibodies (Novus Biologicals). Finally, the membranes were incubated with Pierce ECL Western Blotting Substrate (Thermo Scientific) and read using a ChemiDoc Touch Imaging System (Bio-Rad). Densitometric analysis of bands was performed using Image Lab software (Bio-Rad).

4.9. Statistical analysis

For all experiments, analysis of variance with Tukey’s post-hoc test was performed to assess significant differences across conditions. GraphPad Prism was used to plot the data as mean ± standard deviation. For both 2-D and 3-D culture analysis of ASC phenotypic changes and HUVEC sprouting, at least three replicates were analyzed per condition per experiment; for VEGF secretion, three replicates with a total of six microwells per condition were analyzed. For each study, at least two independent experiments were performed. The level of statistical significance was determined at $p < 0.05$.

Supplementary Material

Refer to Web version on PubMed Central for supplementary material.

Acknowledgments

This work was supported by NIH/NCI (the Cornell Center on the Microenvironment & Metastasis through Award Number U54CA143876 and R01CA185293). Confocal micrographs were acquired using the Cornell BRC-Imaging Facility NIH- S10RR025502. SEM images were taken using the Cornell Center for Materials Research Shared Facilities, which are supported through the NSF MRSEC program (DMR-1120296).

References

1. Chang HY, Nuyten DSA, Sneddon JB, Hastie T, Tibshirani R, Sørlie T, Dai H, He YD, Van LJ, Bartelink H, Van De Rijn M, Brown PO. Robustness, scalability, and integration of a wound-response gene expression signature in predicting breast cancer survival. PNAS. 2005; 102:3738–3743. [PubMed: 15701700]
2. Acerbi I, Cassereau L, Dean I, Shi Q, Au A, Park C, Chen YY, Liphardt J, Hwang ES, Weaver VM. Human breast cancer invasion and aggression correlates with ECM stiffening and immune cell infiltration. Integr Biol. 2015; 7:1120–34.
3. Yamashita M, Ogawa T, Zhang X, Hanamura N, Kashikura Y, Takamura M, Yoneda M, Shiraishi T. Role of stromal myofibroblasts in invasive breast cancer: Stromal expression of alpha-smooth muscle actin correlates with worse clinical outcome. Breast Cancer. 2012; 19:170–176. [PubMed: 20978953]
4. Hinz B, Phan SH, Thannickal VJ, Galli A, Bochaton-Piallat M-L, Gabbiani G. The myofibroblast: one function, multiple origins. Am J Pathol. 2007; 170:1807–16. [PubMed: 17525249]
5. Kalluri R, Zeisberg M. Fibroblasts in cancer. Nat Rev Cancer. 2006; 6:392–401. [PubMed: 16572188]
6. Faouzi S, Le Bail B, Neaud V, Boussarie L, Saric J, Bioulac-Sage P, Balabaud C, Rosenbaum J. Myofibroblasts are responsible for collagen synthesis in the stroma of human hepatocellular carcinoma: an in vivo and in vitro study. J Hepatol. 1999; 30:275–84. [PubMed: 10068108]
7. Paszek MJ, Zahir N, Johnson KR, Lakins JN, Rozenberg GI, Gefen A, Reinhart-King Ca, Margulies SS, Dembo M, Boettiger D, Hammer Da, Weaver VM. Tensional homeostasis and the malignant phenotype. Cancer Cell. 2005; 8:241–54. [PubMed: 16169468]
8. Levental KR, Yu H, Kass L, Lakins JN, Egeblad M, Erler JT, Fong SFT, Csiszar K, Giaccia A, Weninger W, Yamauchi M, Gasser DL, Weaver VM. Matrix crosslinking forces tumor progression by enhancing integrin signaling. Cell. 2009; 139:891–906. [PubMed: 19931152]
9. Lu P, Weaver VM, Werb Z. The extracellular matrix: a dynamic niche in cancer progression. J Cell Biol. 2012; 196:395–406. [PubMed: 22351925]
10. Nicosia RF, Tuszynski GP. Matrix-bound thrombospondin promotes angiogenesis in vitro. J Cell Biol. 1994; 124:183–193. [PubMed: 7507491]
11. Orimo A, Gupta PB, Sgroi DC, Arenzana-Seisdedos F, Delaunay T, Carey VJ, Naeem R, Richardson AL, Weinberg RA. Stromal Fibroblasts Present in Invasive Human Breast Carcinomas Promote Tumor Growth and Angiogenesis through Elevated SDF-1/CXCL12 Secretion. Cell. 2005; 121:335–348. [PubMed: 15882617]
12. Hughes CCW. Endothelial-stromal interactions in angiogenesis. Curr Opin Hematol. 2008; 15:204–9. [PubMed: 18391786]
13. Vong S, Kalluri R. The role of stromal myofibroblast and extracellular matrix in tumor angiogenesis. Genes Cancer. 2011; 2:1139–45. [PubMed: 22866205]
14. Liu F, Mih JD, Shea BS, Kho AT, Sharif AS, Tager AM, Tschumperlin DJ. Feedback amplification of fibrosis through matrix stiffening and COX-2 suppression. J Cell Biol. 2010; 190:693–706. [PubMed: 20733059]
15. Ishii G, Sangai T, Oda T, Aoyagi Y, Hasebe T, Kanomata N, Endoh Y, Okumura C, Okuhara Y, Magae J, Emura M, Ochiya T, Ochiai A. Bone-marrow-derived myofibroblasts contribute to the cancer-induced stromal reaction. Biochem Biophys Res Commun. 2003; 309:232–240. [PubMed: 12943687]

16. Bielli A, Scioli MG, Gentile P, Agostinelli S, Tarquini C, Cervelli V, Orlandi A. Adult adipose-derived stem cells and breast cancer: a controversial relationship. Springerplus. 2014; 3:345. [PubMed: 25089245]
17. Bellows CF, Zhang Y, Simmons PJ, Khalsa AS, Kolonin MG. Influence of BMI on level of circulating progenitor cells. Obesity. 2011; 19:1722–6. [PubMed: 21293449]
18. Cho JA, Park H, Lim EH, Lee KW. Exosomes from breast cancer cells can convert adipose tissue-derived mesenchymal stem cells into myofibroblast-like cells. Int J Oncol. 2012; 40:130–8. [PubMed: 21904773]
19. Jotzu C, Alt E, Welte G, Li J, Hennessy BT, Devarajan E, Krishnappa S, Pinilla S, Droll L, Song Y-H. Adipose tissue derived stem cells differentiate into carcinoma-associated fibroblast-like cells under the influence of tumor derived factors. Cell Oncol. 2011; 34:55–67.
20. Otranto M, Sarrazy V, Bonté F, Hinz B, Gabbiani G, Desmoulière A. The role of the myofibroblast in tumor stroma remodeling. Cell Adhes Migr. 2012; 6:203–219. DOI: 10.4161/cam.20377
21. Wang K, Andresen RC, Wu F, Seo BR, Fischbach C, Gourdon D. Stiffening and unfolding of early deposited-fibronectin increase proangiogenic factor secretion by breast cancer-associated stromal cells. Biomaterials. 2015; 54:63–71. [PubMed: 25907040]
22. Chandler EM, Saunders MP, Yoon CJ, Gourdon D, Fischbach C. Adipose progenitor cells increase fibronectin matrix strain and unfolding in breast tumors. Phys Biol. 2011; 8:015008. [PubMed: 21301062]
23. Zhang Y, Daquinag AC, Amaya-Manzanares F, Sirin O, Tseng C, Kolonin MG. Stromal progenitor cells from endogenous adipose tissue contribute to pericytes and adipocytes that populate the tumor microenvironment. Cancer Res. 2012; 72:5198–208. [PubMed: 23071132]
24. Song YH, Shon SH, Shan M, Stroock AD, Fischbach C. Adipose-derived Stem Cells Increase Angiogenesis through Matrix Metalloproteinase-dependent Collagen Remodeling. Integr Biol. 2016; 8:205–215.
25. Cocucci E, Racchetti G, Meldolesi J. Shedding microvesicles: artefacts no more. Trends Cell Biol. 2009; 19:43–51. [PubMed: 19144520]
26. Santana SM, Antonyak Ma, Cerione Ra, Kirby BJ. Cancerous Epithelial Cell Lines Shed Extracellular Vesicles With a Bimodal Size Distribution that is Sensitive to Glutamine Inhibition. Phys Biol. 2014; 11:65001.
27. Skog J, Würdinger T, van Rijn S, Meijer DH, Gainche L, Sena-Esteves M, Curry WT, Carter BS, Krichevsky AM, Breakefield XO. Glioblastoma microvesicles transport RNA and proteins that promote tumour growth and provide diagnostic biomarkers. Nat Cell Biol. 2008; 10:1470–6. [PubMed: 19011622]
28. Lee TH, D'Asti E, Magnus N, Al-Nedawi K, Meehan B, Rak J. Microvesicles as mediators of intercellular communication in cancer--the emerging science of cellular "debris". Semin Immunopathol. 2011; 33:455–67. [PubMed: 21318413]
29. Giusti I, Ascenzo SD, Millimaggi D, Taraboletti G, Carta G, Franceschini N, Pavan A, Dolo V. Cathepsin B Mediates the pH-Dependent Proinvasive Activity of Tumor-Shed Microvesicles. Neoplasia. 2008; 10:481–488. [PubMed: 18472965]
30. D'Souza-Schorey C, Clancy JW. Tumor-derived microvesicles: shedding light on novel microenvironment modulators and prospective cancer biomarkers. Genes Dev. 2012; 26:1287–99. [PubMed: 22713869]
31. Jorfi S, Ansa-addo EA, Kholia S, Stratton D, Valley S. Inhibition of microvesiculation sensitizes prostate cancer cells to chemotherapy and reduces docetaxel dose required to limit tumor growth in vivo. Sci Rep. 2015:29–39.
32. Grange C, Tapparo M, Collino F, Vitillo L, Damasco C, Deregibus MC, Tetta C, Bussolati B, Camussi G. Microvesicles released from human renal cancer stem cells stimulate angiogenesis and formation of lung premetastatic niche. Cancer Res. 2011; 71:5346–56. [PubMed: 21670082]
33. Pucci F, Pittet MJ. Molecular pathways: tumor-derived microvesicles and their interactions with immune cells in vivo. Clin Cancer Res. 2013; 19:2598–604. [PubMed: 23426276]
34. Paggetti J, Haderk F, Seiffert M, Janji B, Distler U, Ammerlaan W, Kim YJ, Adam J, Lichter P, Solary E, Berchem G, Moussay E. Exosomes released by chronic lymphocytic leukemia cells

induce the transition of stromal cells into cancer-associated fibroblasts. Blood. 2015; 126:1106–1118. [PubMed: 26100252]

35. Cho JA, Park H, Lim EH, Kim KH, Choi JS, Lee JH, Shin JW, Lee KW. Exosomes from ovarian cancer cells induce adipose tissue-derived mesenchymal stem cells to acquire the physical and functional characteristics of tumor-supporting myofibroblasts. Gynecol Oncol. 2011; 123:379–386. [PubMed: 21903249]
36. Desmoulière, a, Geinoz, A., Gabbiani, F., Gabbiani, G. Transforming growth factor-beta 1 induces alpha-smooth muscle actin expression in granulation tissue myofibroblasts and in quiescent and growing cultured fibroblasts. J Cell Biol. 1993; 122:103–111. [PubMed: 8314838]
37. Webber J, Spary L, Sanders A, Chowdhury R, Jiang W, Steadman R, Wymant J, Jones A, Kynaston H, Tabi Z, Clayton A. Differentiation of tumour-promoting stromal myofibroblasts by cancer exosomes. Oncogene. 2014; 34:319–331.
38. Muralidharan-Chari V, Clancy JW, Sedgwick A, D'Souza-Schorey C. Microvesicles: mediators of extracellular communication during cancer progression. J Cell Sci. 2010; 123:1603–1611. [PubMed: 20445011]
39. Kim JB, Stein R, O'Hare MJ. Tumour-Stromal Interactions in Breast Cancer: The Role of Stroma in Tumourigenesis. Tumor Biol. 2005; 26:173–185.
40. Chandler EM, Seo BR, Califano JP, Andresen RC, Lee JS, Yoon CJ, Tims DT, Wang JX, Cheng L, Mohanan S, Buckley MR, Cohen I, Nikitin AY, Williams RM, Gourdon D, Reinhart-King CA, Fischbach C. Implanted adipose progenitor cells as physicochemical regulators of breast cancer. Proc Natl Acad Sci. 2012; 109:9786–9791. [PubMed: 22665775]
41. Bernard K, Logsdon NJ, Ravi S, Xie N, Persons BP, Rangarajan S, Zmijewski JW, Mitra K, Liu G, Darley-Usmar VM, Thannickal VJ. Metabolic reprogramming is required for myofibroblast contractility and differentiation. J Biol Chem. 2015; 290:25427–25438. [PubMed: 26318453]
42. Derynck R, Zhang YE. Smad-dependent and Smad-independent pathways in TGF-beta family signalling. Nature. 2003; 425:577–584. DOI: 10.1038/nature02006 [PubMed: 14534577]
43. Schedin P, Mitrenga T, McDaniel S, Kaeck M. Mammary ECM Composition and function are altered by reproductive state. Mol Carcinog. 2004; 41:207–220. [PubMed: 15468292]
44. Seo BR, Bhardwaj P, Choi S, Gonzalez J, Eguiluz RCA, Wang K, Mohanan S, Morris PG, Du B, Zhou XK, Vahdat LT, Verma A, Elemento O, Hudis CA, Williams RM, Gourdon D, Dannenberg AJ, Fischbach C. Obesity-dependent changes in interstitial ECM mechanics promote breast tumorigenesis. Sci Transl Med. 2015; 7:1–11.
45. Wilson KF, Erickson JW, Antonyak M, Cerione R. Rho GTPases and their roles in cancer metabolism. Trends Mol Med. 2013; 19:74–82. [PubMed: 23219172]
46. Wang J-B, Erickson JW, Fuji R, Ramachandran S, Gao P, Dinavahi R, Wilson KF, Ambrosio ALB, Dias SMG, Dang CV, Cerione Ra. Targeting mitochondrial glutaminase activity inhibits oncogenic transformation. Cancer Cell. 2010; 18:207–19. DOI: 10.1016/j.ccr.2010.08.009 [PubMed: 20832749]
47. De Wever O, Demetter P, Mareel M, Bracke M. Stromal myofibroblasts are drivers of invasive cancer growth. Int J Cancer. 2008; 123:2229–2238. [PubMed: 18777559]
48. Wise DR, Thompson CB. Glutamine Addiction: A New Therapeutic Target in Cancer. Trends Biochem Sci. 2011; 35:427–433.
49. Katt WP, Ramachandran S, Erickson JW, Cerione Ra. Dibenzophenanthridines as Inhibitors of Glutaminase C and Cancer Cell Proliferation. Mol Cancer Ther. 2012; 11:1269–1278. [PubMed: 22496480]
50. Antonyak M, Wilson KF, Cerione Ra. R(h)oads to microvesicles. Small GTPases. 2012; 3:219–24. [PubMed: 22906997]
51. Simpson NE, Tryndyak VP, Pogribna M, Beland Fa, Pogribny IP. Modifying metabolically sensitive histone marks by inhibiting glutamine metabolism affects gene expression and alters cancer cell phenotype. Epigenetics. 2012; 7:1413–1420. [PubMed: 23117580]
52. Altman BJ, Stine ZE, Dang CV. From Krebs to clinic: glutamine metabolism to cancer therapy. Nat Rev Cancer. 2016; 16:619–634. [PubMed: 27492215]

53. Muralidharan-chari V, Clancy J, Plou C, Romao M, Chavrier P. ARF6-Regulated Shedding of Tumor Cell-Derived Plasma Membrane Microvesicles. Curr Biol. 2009; 19:1875–1885. [PubMed: 19896381]
54. Raposo G, Stoorvogel W. Extracellular vesicles: Exosomes, microvesicles, and friends. J Cell Biol. 2013; 200:373–383. [PubMed: 23420871]
55. Kis K, Liu X, Hagood JS. Myofibroblast differentiation and survival in fibrotic disease. Expert Rev Mol Med. 2011; 13:e27. [PubMed: 21861939]
56. Wan AMD, Chandler EM, Madhavan M, Infanger DW, Ober CK, Gourdon D, Malliaras GG, Fischbach C. Fibronectin conformation regulates the proangiogenic capability of tumor-associated adipogenic stromal cells. Biochim Biophys Acta. 2013; 1830:4314–20. [PubMed: 23567798]
57. Caraci F, Gili E, Calafiore M, Failla M, La Rosa C, Crimi N, Sortino MA, Nicoletti F, Copani A, Vancheri C. TGF-B1 targets the GSK-3B/B-catenin pathway via ERK activation in the transition of human lung fibroblasts into myofibroblasts. Pharmacol Res. 2008; 57:274–282. [PubMed: 18346908]
58. De Wever O, Westbroek W, Verloes A, Bloemen N, Bracke M, Gespach C, Bruyneel E, Mareel M. Critical role of N-cadherin in myofibroblast invasion and migration in vitro stimulated by colon-cancer-cell-derived TGF-beta or wounding. J Cell Sci. 2004; 117:4691–4703. [PubMed: 15331629]
59. Sapudom J, Rubner S, Martin S, Thoenes S, Anderegg U, Pompe T. The interplay of fibronectin functionalization and TGF-β1 presence on fibroblast proliferation, differentiation and migration in 3D matrices. Biomater Sci. 2015; 3:1291–301. [PubMed: 26230292]
60. Kimura H, Okubo N, Chosa N, Kyakumoto S, Kamo M, Miura H, Ishisaki A. EGF positively regulates the proliferation and migration, and negatively regulates the myofibroblast differentiation of periodontal ligament-derived endothelial progenitor cells through MEK/ERK-and JNK-dependent signals. Cell Physiol Biochem. 2013; 32:899–914. [PubMed: 24217646]
61. Desai VD, Hsia HC, Schwarzbauer JE. Reversible modulation of myofibroblast differentiation in adipose-derived mesenchymal stem cells. PLoS One. 2014; 9:1–12.
62. Zhou X, Rowe RG, Hiraoka N, George JP, Wirtz D, Mosher DF, Virtanen I, Chernousov MA, Weiss SJ. Fibronectin fibrillogenesis regulates three-dimensional neovessel formation. Genes Dev. 2008; 22:1231–1243. [PubMed: 18451110]
63. Kanada M, Bachmann MH, Contag CH. Signaling by Extracellular Vesicles Advances Cancer Hallmarks. Trends in Cancer. 2016; 2:84–94.
64. Zhao M, Wang X, Dumur CI, Idowu MO, Robila V, Francis M, Ware J, Beckman M, Lynne W. Mesenchymal stem cells in mammary adipose tissue stimulate progression of breast cancer resembling the basal-type. Cancer Biol Ther. 2012; 13:782–792. [PubMed: 22669576]
65. Huang X, Yang N, Fiore VF, Barker TH, Sun Y, Morris SW, Ding Q, Thannickal VJ, Zhou Y. Matrix stiffness-induced myofibroblast differentiation is mediated by intrinsic mechanotransduction. Am J Respir Cell Mol Biol. 2012; 47:340–348. [PubMed: 22461426]
66. Dvorak HF. How tumors make bad blood vessels and stroma. Am J Pathol. 2003; 162:1747–57. [PubMed: 12759232]
67. Seo BR, DelNero P, Fischbach C. In vitro models of tumor vessels and matrix: Engineering approaches to investigate transport limitations and drug delivery in cancer. Adv Drug Deliv Rev. 2014; 69–70:205–216.
68. Chwalek K, Bray LJ, Werner C. Tissue-engineered 3D tumor angiogenesis models: Potential technologies for anti-cancer drug discovery. Adv Drug Deliv Rev. 2014; 79:30–39. [PubMed: 24819220]
69. Verbridge SS, Choi NW, Zheng Y, Brooks DJ, Stroock AD, Fischbach C. Oxygen-controlled three-dimensional cultures to analyze tumor angiogenesis. Tissue Eng Part A. 2010; 16:2133–41. [PubMed: 20214469]

Highlights

- Tumor extracellular vesicles (TEVs) convert adipose stem cells (ASCs) into myofibroblasts.
- Mitogen-activated protein kinase signaling-plays a role in this process.
- Blocking glutamine metabolism inhibits TEV formation and subsequent transformation of ASCs.
- TEV-treated ASCs exhibit increased VEGF secretion and extracellular matrix remodeling.
- TEV-mediated angiogenic changes of ASCs promote endothelial sprouting.

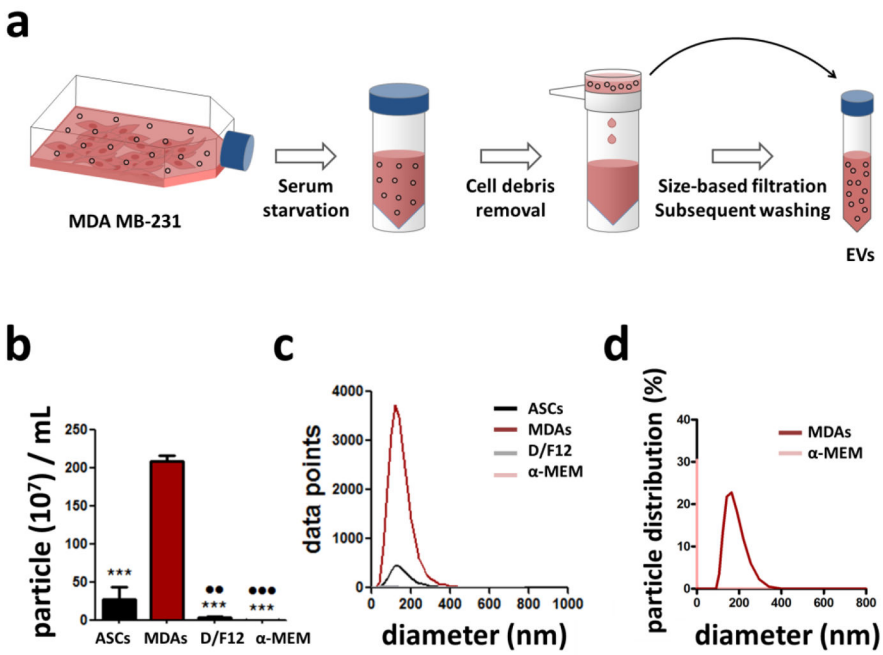

Figure 1. Collection and characterization of extracellular vesicles (EVs)

a) Subconfluent MDA MB-231 (MDAs) were subjected to serum starvation for 7–12 hours. Media was harvested, centrifuged to remove cell debris, and then filtered to enrich for EVs. This EV fraction was then used for subsequent experiments and analyses. Control media was prepared by placing serum-free media in the incubator and processing it similarly. b) Concentration of particles in the blank control media *vs.* ASC- and MDA-derived EVs as measured by NanoSight. ***p<0.001 vs. MDAs, ●● p<0.01 vs. ASCs, and ●●● p<0.001 vs. ASCs c) Size distribution of particles in the blank control media *vs.* ASC- and MDA-derived EVs as measured by NanoSight. d) Particle size distribution in blank control media vs. MDA-conditioned media as measured by Zetasizer.

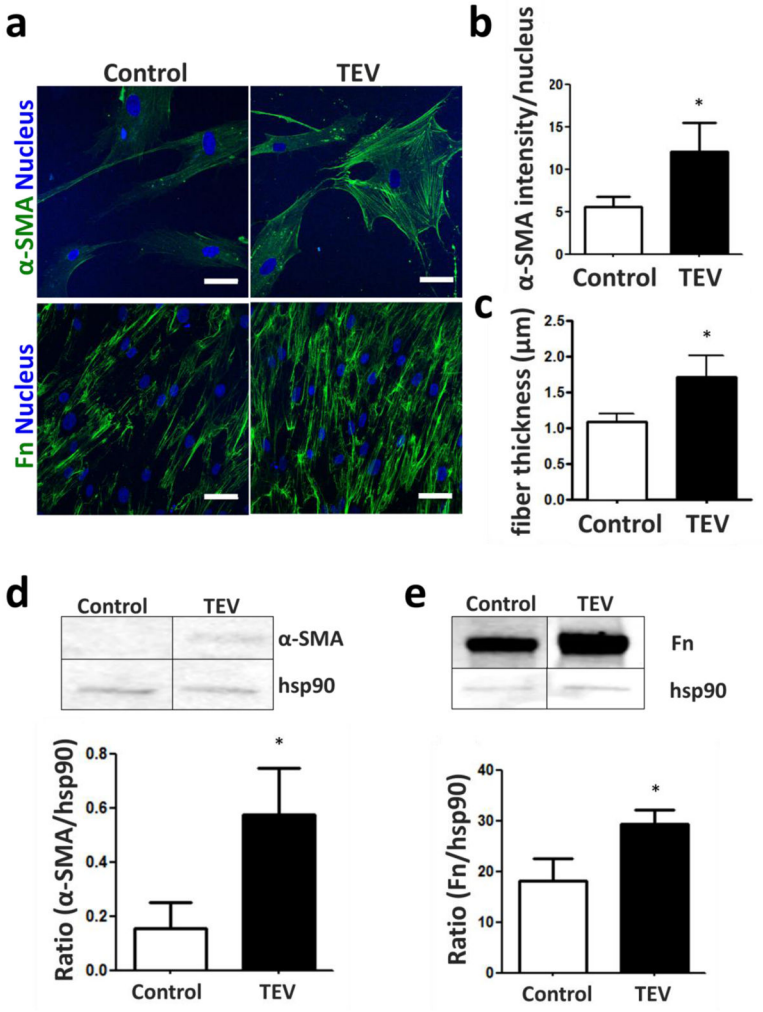

Figure 2. Myofibroblastic marker expression of ASCs in 2-D is enhanced with TEV treatment

a) α-SMA and fibronectin (Fn) of ASCs treated with or without tumor cell-derived EVs (TEVs) as visualized by immunofluorescence. Scale bar = 50 um. b) Quantification of α-SMA levels and c) Fn fiber thickness by image analysis. d), e) Western blots and corresponding densitometric analyses of α-SMA and Fn. * $p<0.05$.

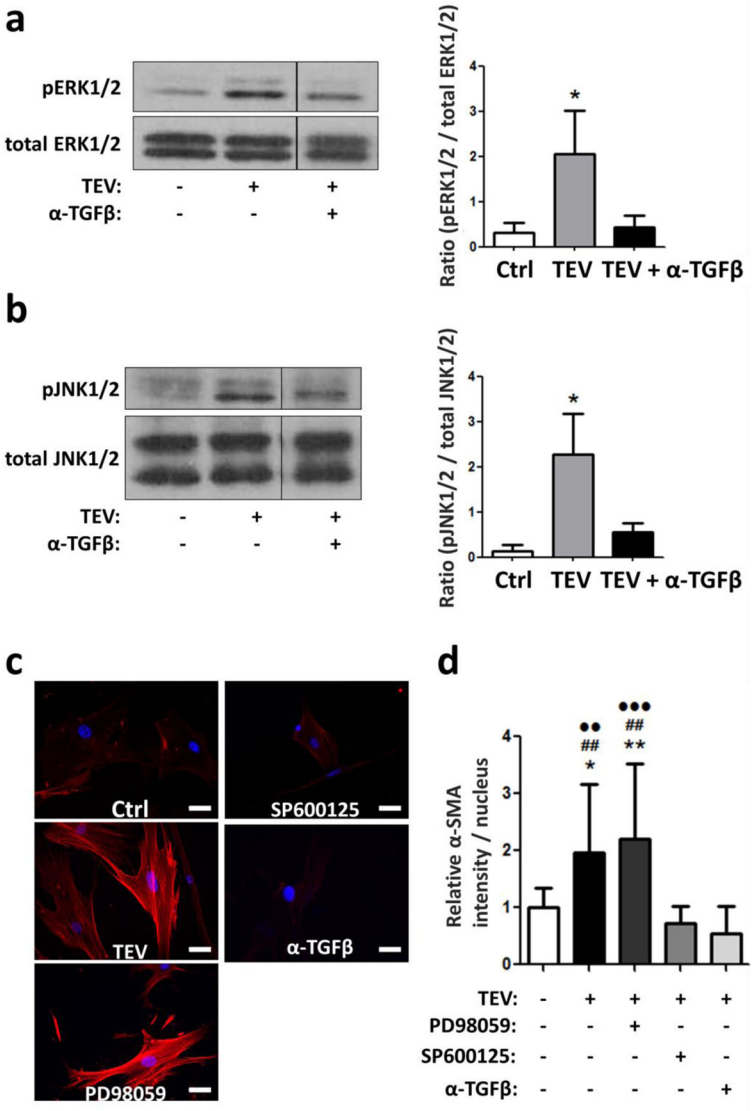

Figure 3. TEV treatment of ASCs activates MAPK signaling

Western blots and densitometric analysis of phosphorylated and total ERK (a) and JNK (b). * $p<0.05$ *vs.* all other conditions. c) Immunofluorescence of α-SMA (red) and nuclei (blue) of ASCs treated with TEVs in the presence and absence of a function-blocking TGF-β antibody (α-TGFβ), the MEK inhibitor PD98059, and the JNK inhibitor SP600125. Scale bar = 50 um. d) Quantification of α-SMA levels by image analysis. * $p<0.05$ vs. Ctrl, # $p<0.05$ vs. α-TGFβ, ● $p<0.05$ vs. SP600125. One, two, and three symbols indicate $p<0.05$, $p<0.01$, and $p<0.001$, respectively.

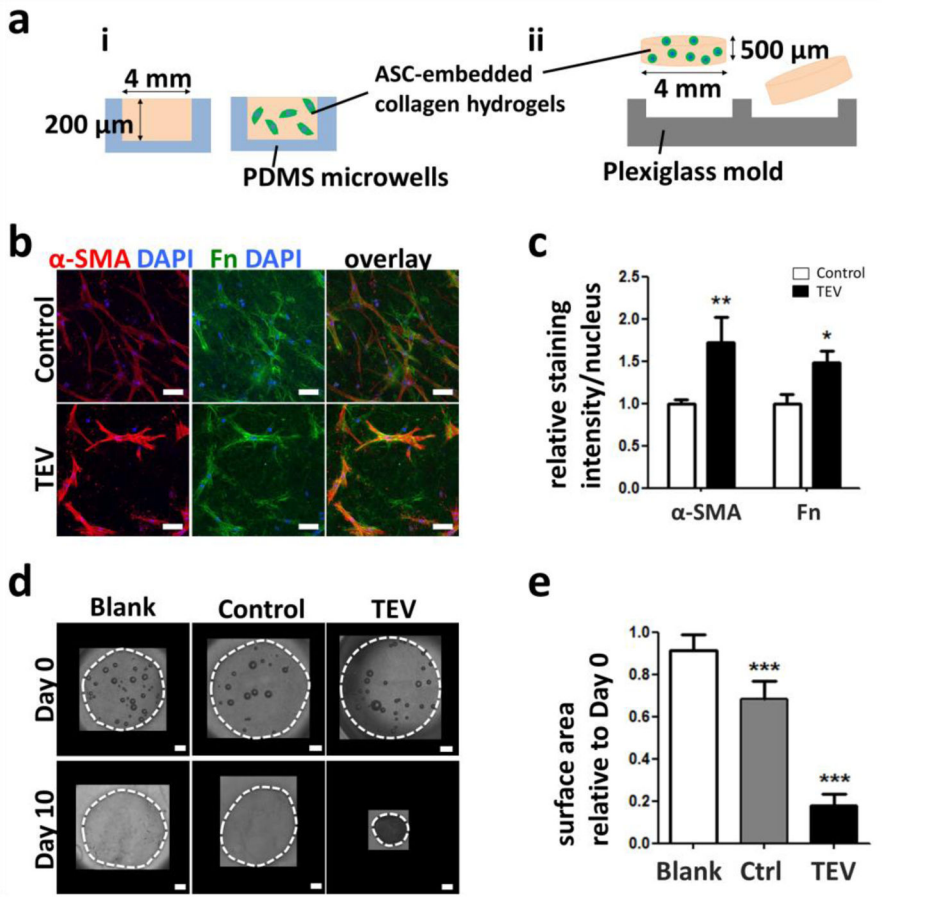

Figure 4. TEV treatment increases ASCs myofibroblastic behavior in 3-D culture

a) Schematic of 3-D culture systems: i) PDMS microwells and ii) free-floating collagen disks. b) Confocal micrographs of ASC α-SMA and Fn immunofluorescence following culture in collagen-based microwell cultures. Scale bar = 50 µm. c) Corresponding image analysis of immunofluorescence. * $p<0.05$ and ** $p<0.01$ *vs.* respective controls. d) Micrographs of free-floating 3-D collagen disks seeded with ASCs and cultured with control media or TEVs at day 0 and day 10. Blank collagen disks are shown as controls. Dotted white lines mark the gels. Scale bar = 500 µm. e) Relative changes in surface area of the disks at day 10. *** $p<0.001$ *vs.* all other conditions.

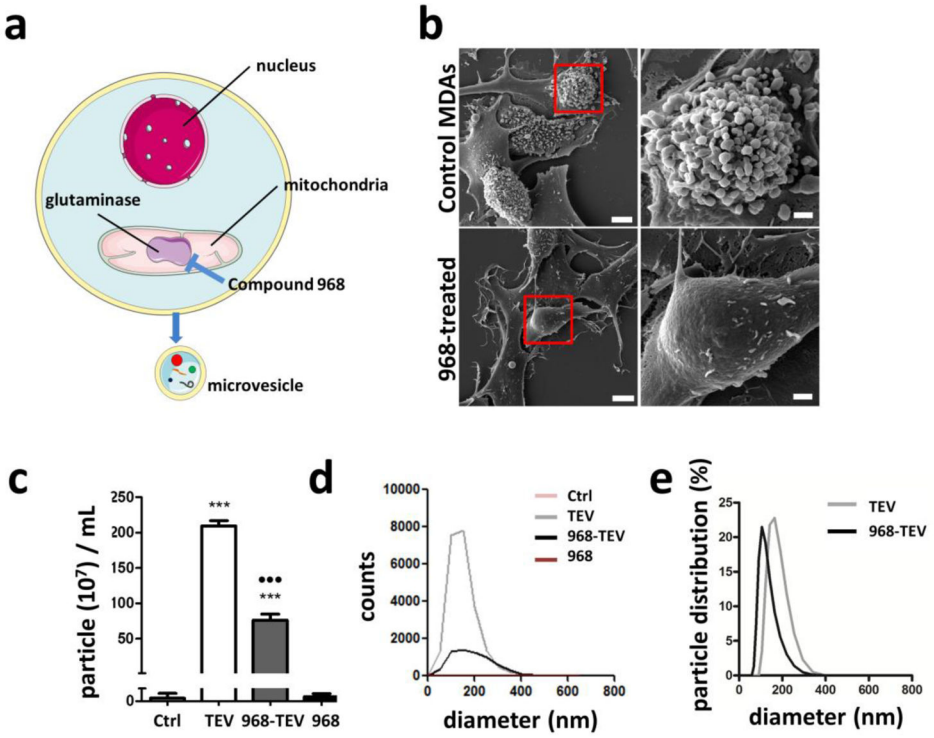

Figure 5. Inhibition of glutaminase with compound 968 reduces TEV formation by MDAs

a) Schematic (adapted from Servier Medical Art) showing mechanism of compound 968 inhibiting TEV biogenesis. b) SEM images of MDAs treated with or without 968. For each condition, a higher magnification image of the red-boxed area is shown on the right. Lower magnification scale bar = 5 μm, and higher magnification scale bar = 1 μm. c) Particle concentration in media collected from MDAs (TEV) and 968-treated MDAs (968-TEV) as well as respective control media as analyzed by NanoSight. *** $p<0.001$ *vs.* Control and 968. ●●● $p<0.001$ *vs.* TEV. d) Corresponding particle size distribution as measured by NanoSight. e) Particle size distribution from TEVs and 968-TEVs, as measured by Zetasizer.

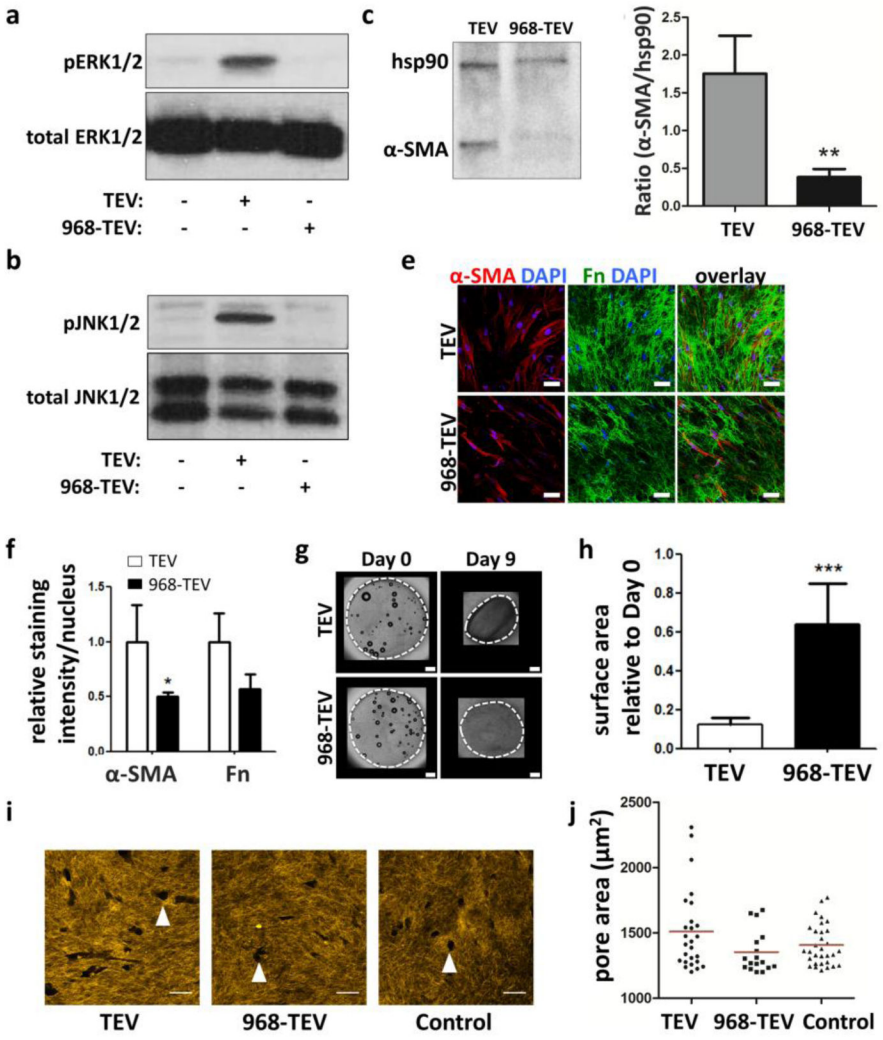

Figure 6. TEVs collected from 968-treated MDAs reduce ASC myofibroblastic behavior

Phosphorylated and total levels of (a) JNK1/2 and (b) ERK1/2 from ASCs treated with TEVs from control MDAs (TEV) *vs.* 968-treated MDAs (968-TEV). c) Confocal micrographs of α-SMA and Fn levels of ASCs treated with TEVs *vs.* 968-TEVs. Scale bar = 50 μm. d) Image analysis of α-SMA and Fn immunofluorescence intensity. * $p<0.05$ *vs.* TEVs α-SMA. e, f) Western blots and corresponding densitometric quantification of α-SMA and Hsp90 from ASCs treated with TEVs and 968-TEVs. g) Representative images of day 0 and day 9 ASC-embedded collagen disks treated with TEVs *vs.* 968-TEVs. Dotted white lines mark the gels. Scale bar = 500 μm. h) Quantification of surface area changes relative to day 0. *** $p<0.001$. i) Representative confocal reflectance images of collagen matrices embedded with TEV, 968-TEV, and control media-treated ASCs. Arrowheads indicate degradation pores created by ASCs. Scale bar = 50 μm. j) Distribution of pore areas. Red lines indicate mean values.

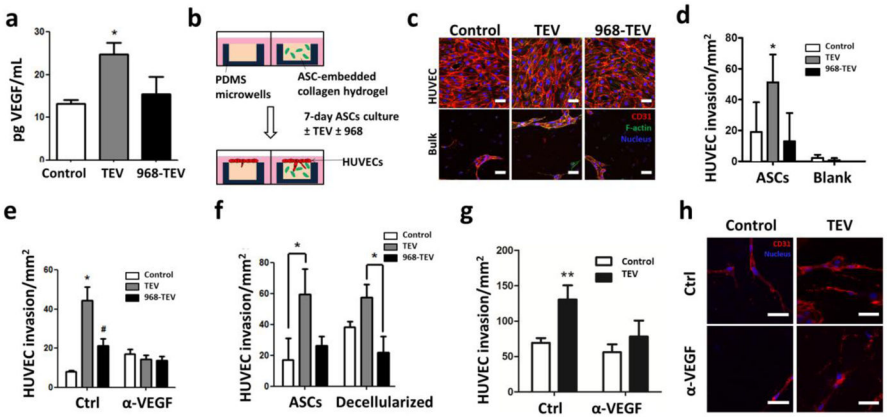

Figure 7. TEV-pretreatment stimulates the pro-angiogenic capability of ASCs

a) VEGF secretion of control ASCs and ASCs treated with TEVs and 968-TEVs as measured by ELISA. * $p<0.05$ *vs.* all other conditions. b) Schematic of endothelial cell invasion assay. c) Confocal micrographs of ASC/HUVEC co-cultures in 3-D microwells following immunofluorescent staining for CD31. Representative confocal slices of the HUVEC monolayer and sprouts within the bulk are shown. Scale bar = 50 μm. d) Corresponding quantification of HUVEC sprouts via image analysis. * $p<0.05$ *vs.* TEV, ASCs. e) Quantification of HUVEC sprouts in the presence of a VEGF neutralizing antibody. * $p<0.05$ *vs.* all other conditions, # $p<0.05$ *vs.* Ctrl/Control. f) Quantification of HUVEC sprouts into ASC-embedded or decellularized microwells. * $p<0.05$. g) Quantification of HUVEC sprouts within decellularized collagen gels in the absence and presence of a VEGF neutralizing antibody. ** $p<0.01$ *vs.* all other conditions. h) Confocal micrographs of HUVEC sprouts within decellularized microwells. Scale bar = 50 μm.